analytical chemistry

Letter

pubs.acs.org/ac

Imaging of Proteins in Tissue Samples Using Nanospray Desorption Electrospray Ionization Mass Spectrometry

Cheng-Chih Hsu,[†,‡] Pi-Tai Chou,[‡] and Richard N. Zare*[,†]

[†]Department of Chemistry, Stanford University, Stanford, California 94305, United States

[‡]Department of Chemistry, National Taiwan University, Taipei 10617, Taiwan

Supporting Information

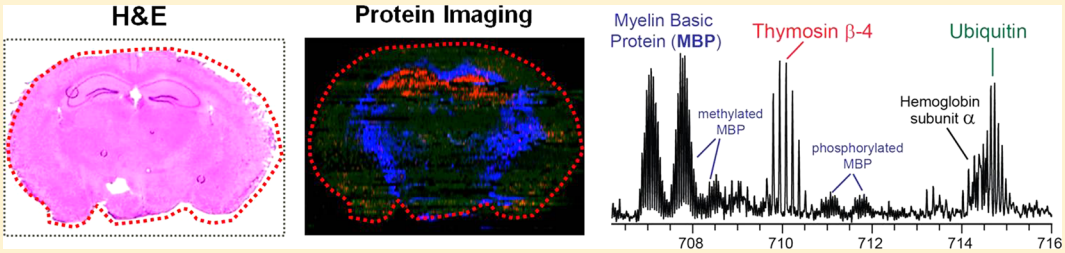

ABSTRACT: Chemical maps of tissue samples provide important information on biological processes therein. Recently, advances in tissue imaging have been achieved using ambient ionization techniques, such as desorption electrospray ionization mass spectrometry (DESI-MS), but such techniques have been almost exclusively confined to the mapping of lipids and metabolites. We report here the use of nanospray desorption electrospray ionization (nanoDESI) that allows us to image proteins in tissue samples in a label-free manner at atmospheric pressure with only minimum sample preparation. Multiply charged proteins with masses up to 15 kDa were successfully detected by nanoDESI using an LTQ Orbitrap mass spectrometer. In an adult mice brain section, expression of proteins including ubiquitin, β-thymosin, myelin basic protein, and hemoglobin were spatially mapped and characterized. We also determined the location of methylation on myelin basic protein. This imaging modality was further implemented to MYC-induced lymphomas. We observed an array of truncated proteins in the region where normal thymus cells were infiltrated by tumor cells, in contrast to healthy tissue.

Numerous mass spectrometry imaging (MSI) modalities allowing analysis of intact biomolecules have been implemented to biological systems.[1] Among these MSI techniques, matrix-assisted laser desorption ionization (MALDI) is widely used for protein imaging,[2,3] and proteins of up to 80 kDa or higher can be spatially resolved and analyzed directly on animal samples, such as brain and tumor sections.[4−6] However, MALDI imaging is limited by three considerations: (1) it usually takes hours of sample preparation because an evenly deposited layer of crystallized organic matrix on sample surfaces is required; (2) high vacuum environments are usually used for MALDI, although scanning MALDI operations under ambient conditions have been reported by Spengler and co-workers;[7] and (3) MALDI often suffers from interferences from the presence of the matrix.

An alternative approach that allows soft ionization under atmospheric pressure has been developed during the past decade. The greatest advantage of this approach is that samples do not require matrix deposition, so that tissue sections can be directly investigated by mass spectrometry in the open air.[8−10] Among ambient ionization methods for this purpose, desorption electrospray ionization (DESI) is most commonly used. DESI utilizes a high-speed charged microdroplet spray to desorb analytes directly from sample surfaces, so as to obtain distributions of metabolites and lipid species in tissues.[11] Because a biological sample remains intact even after mass spectrometric interrogation, DESI MSI is further applied to pathological evaluation of diseases, e.g., cancer, based on molecular signatures in the tissue.[12−16]

However, DESI MSI has been unable to obtain signals from proteins in biological tissue sections. In fact, this limitation takes place in most of the ambient ionization methods. Recently, several groups have shown that with improved ion/sample transport, proteins as large as 15 kDa can be analyzed using ambient ionization mass spectrometry directly on the surface without enzymatic digestions.[17−20] One of these methods is nanospray desorption electrospray ionization (nanoDESI).[21,22] In nanoDESI, the charged microdroplet spray in DESI is substituted with a capillary tube applied with high voltage and with continuous solvent infusion to mobilize compounds via microextraction from sample surfaces. Solvated analytes are aspirated by a second capillary tube and the subsequent electrospray ionization occurs at the outlet of the second capillary tube. In a previous study, Hsu et al. interfaced nanoDESI MS with an inverted microscope for protein imaging, spot by spot.[17] However, this microscopy-

Received: September 5, 2015
Accepted: October 28, 2015
Published: October 28, 2015

DOI: 10.1021/acs.analchem.5b03389
Anal. Chem. 2015, 87, 11171−11175

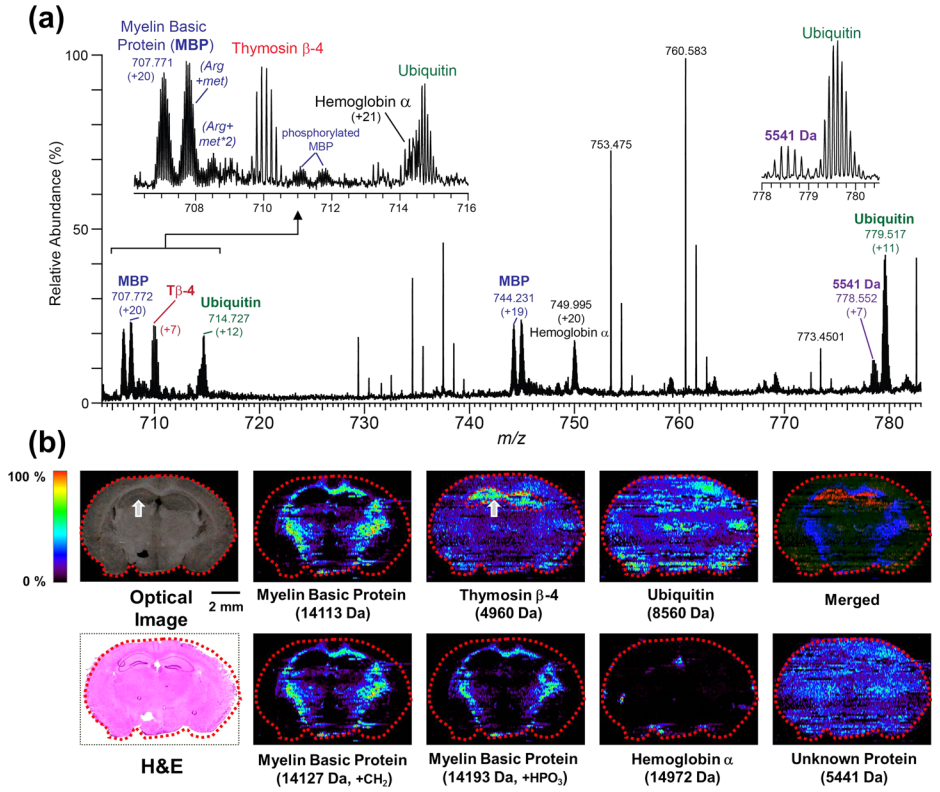

Figure 1. (a) Representative positive ion mode mass spectra of proteins in a 20-μm thick adult mice brain coronal section. Isotopic distributions of each protein are resolved as in the zoomed-in spectra. Unmarked peaks are unwashed lipids. (b) Molecular imaging of proteins in adult mice brain section. Optical image in the upper panel is the same section slide after lipid wash. An adjacent slide was subject to H&E stain for comparison. The arrow indicates hippocampus of the brain. Merged image: MBP (blue), thymosin β-4 (red), and ubiquitin (green).

guided approach is not efficient especially when imaging larger tissue sections. Here we further demonstrate that nanoDESI MSI is capable of label-free protein imaging in tissues at atmospheric pressure with only minimum sample preparation by mounting the slide of tissue sections on an $X-Y$ translation stage, the same way as was previously done for lipids and metabolites (see Figure S1).[21,22] We present two-dimensional (2D) MS images of mice brain and MYC-induced lymphoma tissue sections which have allowed us to visualize endogenous proteins in substructures.

Details of the characterization of the nanoDESI detection response are presented in the Supporting Information. As shown in Figure S2, acceptable linearity of calibration curves was obtained for both cytochrome c and insulin. A limit of detection (LOD) of ~20 pmol/mg (for tissue homogenates) was achieved, which is sufficient to cover many high abundance proteins in cells.

We modified the platform previously used for DESI MSI in our laboratory for nanoDESI MSI in this study.[16] Frozen tissues were sectioned into 20-μm slices without any fixation. Tissue sections were slightly rinsed with 10 μL of chloroform twice (5 s each) before MS interrogation to reduce ion suppression by endogenous lipid species. Ions were introduced to the LTQ Orbitrap to obtain high resolution mass spectra. Protein ions were analyzed using top-down tandem mass spectrometry (ProSight PTM).[23] Detailed experimental methods and setup are described in the Supporting Information.

Many proteins are known to be heterogeneously distributed within different brain regions and structures. We used an adult mouse section for nanoDESI MS imaging. Figure 1a shows an averaged mass spectrum obtained from a row of data acquired across the hippocampus of the mouse brain (Figure 1b). For this m/z region, an array of multiply charged macromolecules were clearly observed in positive ion mode. These macromolecules were later identified using tandem mass spectrometry as ubiquitin, thymosin β-4, hemoglobin, and myelin basic proteins (MBPs). The Orbitrap is able to resolve isotopic patterns enabling mass deconvolution. The monoisotopic masses of each species are listed in Figure 1b. We present 2D nanoDESI MS images of specific protein species observed within the mouse brain section. The majority of the ions in the gray matter are MBPs, e.g., m/z 707.071 (+20 charges, MW = 14 113.1 Da), and the subsequent images show complementary spatial resolution revealing distinctive features of gray matter in the brain, which is known to consist of considerable amounts of myelinated axons. A second imaging focus on hippocampus region is shown in Supporting Information (Figure S11), and the result indicates the achievement of a lateral spatial resolution of ≈200 μm for protein imaging.

The high resolving power of Orbitrap allows us to capture and distinguish mass differences of MBPs derived from post-translational modification (PTM). A distinct cluster of ions at m/z 707.772 (+20 charge, MW = 14 127.1 Da), observed at a similar level as unmodified MBP at m/z 707.071, is ascribed to methylated MBP (*met*-MBP). It has been reported that an arginine of MBPs, in the sequence Lys-Gly-^{104}Arg-Gly-Leu, can potentially be enzymatically catalyzed into methylated derivatives.[24] This monomethylarginine at residue-104 was further confirmed by MS/MS (Figure S3). Similar spatial distributions were also observed for ion clusters at m/z 708.469, 711.068, 711.771 (+20 charge for all), and these are putatively assigned to MBPs with dimethylarginine (14 141.2 Da), phosphorylated

DOI: 10.1021/acs.analchem.5b03389
Anal. Chem. 2015, 87, 11171−11175

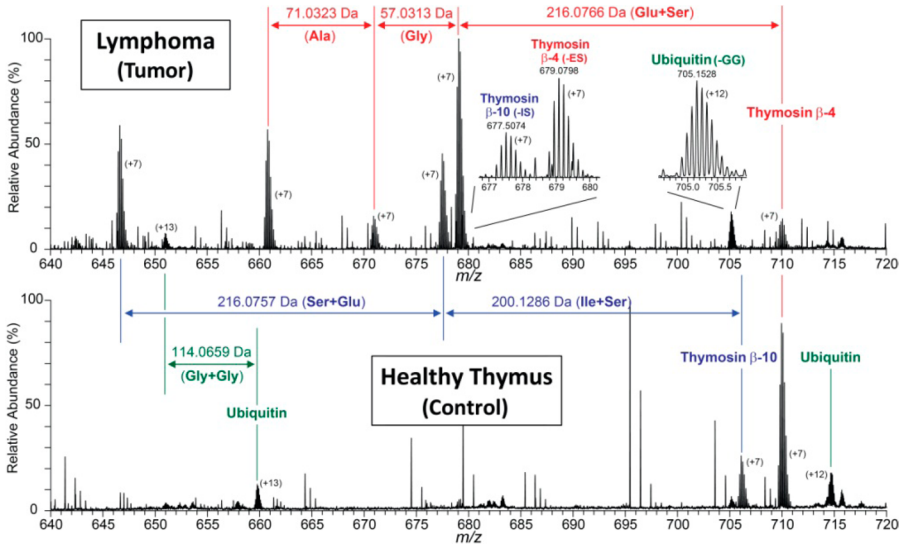

Figure 2. Representative nanoDESI-MS mass spectra in positive ion mode showing alteration of protein profiles in MYC-induced lymphomas. Data were acquired on 15-μm thick mouse tissue sections of healthy thymus and lymphoma. Missing of C-terminal amino acid residues in each truncated proteins are revealed by the shifts of molecular weights corresponding to the intact protein species. Unmarked peaks are unwashed lipids and optimal cutting temperature (OCT) compounds.

MBP (14 193.2 Da), and phosphorylated MBP with monomethylarginine (14 207.2 Da), respectively.

As shown in Figure 1a, the other proteins, such as ubiquitin and a protein with monoisotopic mass 5440.8 Da, were found homogeneously distributed throughout the brain section. On the contrary, the actin-sequestering protein thymosin β-4 was found at high relative intensity in the hippocampus and at a relatively lower intensity in the other regions of the brain. This result is in agreement with other reports that were validated at the nucleotide level.[25] Hemoglobin subunit α was also observed and possibly reveals the distribution of major blood vessels in the brain. In general, the signals of proteins outside the tissue section area are almost negligible, implying that the lipid washing step does not result in much image distortion.

Molecular profiling using MSI has become a mechanism to interrogate the diseases states of cancers.[13−16,26,27] In our laboratory, using DESI MSI we captured alterations of lipid profiles in MYC-induced lymphomas and showed that such molecular changes can be used to predict with high confidence the presence of disease states on morphological regions of tumor sections.[16] We implemented nanoDESI MSI to determine if such molecular changes also occur at the protein level. Frozen tissue sections of lymphomas and healthy lymph nodes collected for our previous DESI MSI investigation were subject to protein imaging in this study by nanoDESI MS. Two distinctive mass spectral patterns were obtained in positive ion mode offering a direct comparison of protein profiles depending on the whether MYC is turned on or not (Figure 2). In healthy thymus, the majority of protein ions observed in the mass spectra correspond to ubiquitin (m/z 714.657), thymosin β-4 (m/z 709.950), and β-10 (m/z 706.097) with full lengths of sequences. Meanwhile, a more complicated mass spectral profile containing many more protein species is detected in the lymphoma tissue in contrast to the healthy thymus tissue section. We listed the masses of all the ions in the lymphoma and compared with the molecular weights of proteins in the healthy section. As shown in Figure 2, some of the ion pairs render the mass shifts that are in accordance with the molecular weights of C-terminal residues of the full-length protein. These shifts imply losses of amino acid tags, including ^{42}Glu-Ser and ^{40}Ala-Gly-Glu-Ser in thymosin β-4, ^{42}Ile-Ser and ^{40}Gly-Gly-Ile-Ser in thymosin β-10, as well as ^{75}Gly-Gly in ubiquitin at the carboxy-terminal. Top-down MS/MS results verify explicitly these assignments (see Figure 3 and the Supporting Information).

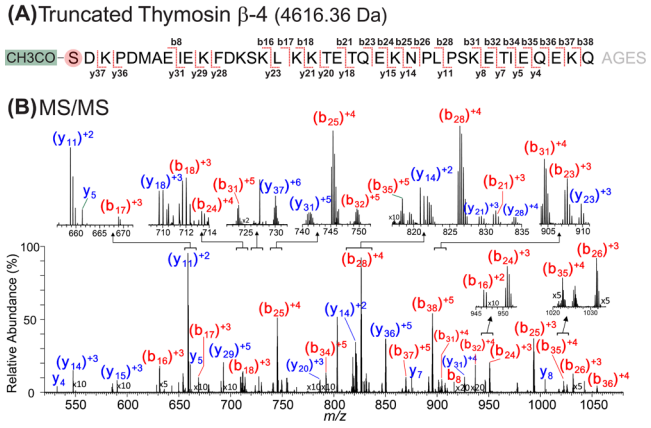

Figure 3. Top-down analysis of truncated thymosin β-4. Proteins were ionized directly on tissue sections using nanoDESI for subsequent collision-induced dissociation. (A) Fragmentation map of the truncated thymosin β-4. The missing amino acid residues in the C-terminal are shown in gray. (B) Annotated MS/MS spectrum.

Mappings of these proteins using nanoDESI MSI provides a powerful tool complementary to immunohistology. Figure 4 clearly reveals that the intact proteins are highly abundant in healthy tissue in most of the thymus cells except for connective tissues and fat cells. In contrast, truncated protein species are dominant in lymphoma exhibiting a significant spatial heterogeneity. To gain more insight into the biased distribution and determine if it is associated with a certain phenotypic pattern, an adjacent slide was stained using standard hematoxylin and eosin (H&E) for further pathological evaluation. Interestingly, the MYC-ON section contained

DOI: 10.1021/acs.analchem.5b03389
Anal. Chem. 2015, 87, 11171−11175

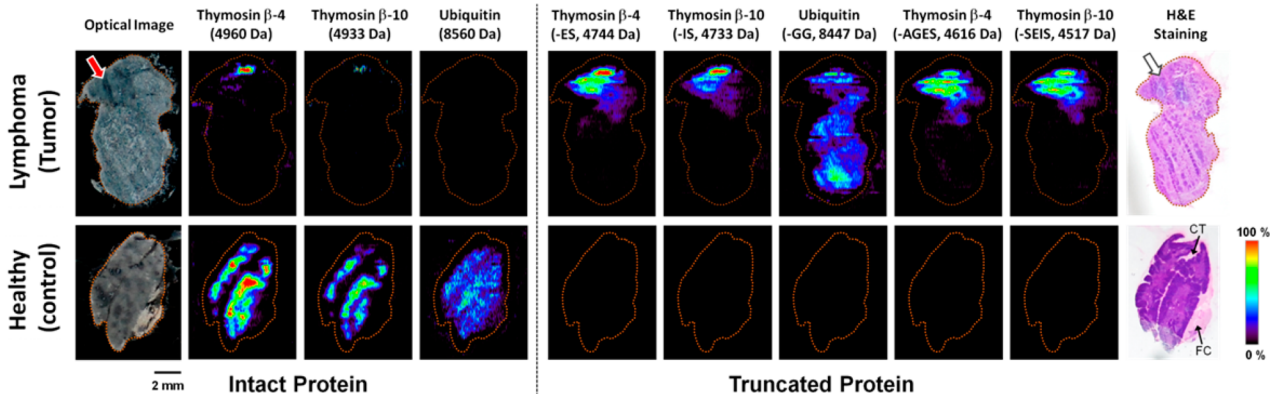

Figure 4. Molecular imaging of proteins in MYC-induced lymphoma and healthy thymus sections using nanoDESI MSI. Truncated forms of proteins were largely found in the tumor particularly the region where normal thymus cells were infiltrated by cancerous cells (arrow). *FC*: fat cells. *CT*: connective tissues.

normal thymus cells in a region that was being infiltrated by tumor cells. This substructure, where normal cells and tumor cells coexist, constitutes the darker region that can be seen by optical images (Figure 4). The MSI images indicate that truncated β-thymosins were highly expressed in the coexistence region, in contrast to the normal thymus section and regions of purely tumor cells on the same slide. Discovery of damaged proteins in lymphoma is not surprising. In fact, modified C-terminal forms of ubiquitin and β-thymosins have been reported in other types of cancers using MALDI MSI and are thought to be associated with tumor aggressiveness and proliferation.[26,27]

More importantly, such cleavage in the C-terminal residues is difficult to be measured by immuno-based techniques commonly used in many biochemistry studies. As most of the affinity interaction requires only a small portion of sequences, proteins with minor changes in few terminal residues will be nonspecifically recognized by the antibody. As a result, alteration of protein profiles, in the context of defect tail in molecules, will very likely escape detection. This highlights the usefulness of nanoDESI MSI coupling with a high-resolution mass analyzer, as it enables a rapid detection of protein expression patterns in a top-down manner. In conclusion, we have presented a new methodology for visualizing proteins of modest molecular weight in tissue sections using a readily implemented ambient ionization technique. It is expected that this new tool will provide important biological insight into cellular processes.

■ ASSOCIATED CONTENT

Supporting Information

The Supporting Information is available free of charge on the ACS Publications website at DOI: 10.1021/acs.analchem.5b03389.

Experimental details and supporting figures (PDF)

■ AUTHOR INFORMATION

Corresponding Author

*E-mail: zare@stanford.edu.

Notes

The authors declare no competing financial interest.

■ ACKNOWLEDGMENTS

C.-C. Hsu is grateful to Ministry of Science and Technology, Taiwan, (MOST) for his financial support. We thank Richard Luong (Department of Comparative Medicine, Stanford University) for the pathology services. We thank the Felsher group (Department of Medicine, Stanford University) and Dr. Livia Eberlin for lymphoma samples and other support. This work was supported by NIH Grant 1R01CA184384-01.

■ REFERENCES

(1) Spengler, B. *Anal. Chem.* **2015**, *87*, 64−82.
(2) Caprioli, R. M.; Farmer, T. B.; Gile, J. *Anal. Chem.* **1997**, *69*, 4751−4760.
(3) Van de Plas, R.; Yang, J.; Spraggins, J.; Caprioli, R. M. *Nat. Methods* **2015**, *12*, 366−372.
(4) Seeley, E. H.; Caprioli, R. M. *Proc. Natl. Acad. Sci. U. S. A.* **2008**, *105*, 18126−18131.
(5) Caprioli, R. M. *Cancer Res.* **2005**, *65*, 10642.
(6) Chaurand, P.; Norris, J. L.; Cornett, D. S.; Mobley, J. A.; Caprioli, R. M. *J. Proteome Res.* **2006**, *5*, 2889−2900.
(7) Bhandari, D. R.; Schott, M.; Römpp, A.; Vilcinskas, A.; Spengler, B. *Anal. Bioanal. Chem.* **2015**, *407*, 2189−2201.
(8) Monge, M. E.; Harris, G. A.; Dwivedi, P.; Fernández, F. M. *Chem. Rev.* **2013**, *113*, 2269−2308.
(9) Badu-Tawiah, A. K.; Eberlin, L. S.; Ouyang, Z.; Cooks, R. G. *Annu. Rev. Phys. Chem.* **2013**, *64*, 481−505.
(10) Hsu, C.-C.; Dorrestein, P. C. *Curr. Opin. Biotechnol.* **2015**, *31*, 24−34.
(11) Wiseman, J. M.; Puolitaival, S. M.; Takáts, Z.; Cooks, R. G.; Caprioli, R. M. *Angew. Chem., Int. Ed.* **2005**, *44*, 7094−7097.
(12) Eberlin, L. S.; Ferreira, C. R.; Dill, A. L.; Ifa, D. R.; Cheng, L.; Cooks, R. G. *ChemBioChem* **2011**, *12*, 2129−2132.
(13) Perry, R. H.; Bellovin, D. I.; Shroff, E. H.; Ismail, A. I.; Zabuawala, T.; Felsher, D. W.; Zare, R. N. *Anal. Chem.* **2013**, *85*, 4259−4262.
(14) Eberlin, L. S.; Tibshirani, R. J.; Zhang, J.; Longacre, T. A.; Berry, G.; Bingham, D. B.; Norton, J. A.; Zare, R. N.; Poultsides, G. A. *Proc. Natl. Acad. Sci. U. S. A.* **2014**, *111*, 2436−2441.
(15) Abbassi-Ghadi, N.; Veselkov, K.; Kumar, S.; Huang, J.; Jones, E.; Strittmatter, N.; Kudo, H.; Goldin, R.; Takáts, Z.; Hanna, G. B. *Chem. Commun.* **2014**, *50*, 3661−3664.
(16) Eberlin, L. S.; Gabay, M.; Fan, A. C.; Gouw, A. M.; Tibshirani, R. J.; Felsher, D. W.; Zare, R. N. *Proc. Natl. Acad. Sci. U. S. A.* **2014**, *111*, 10450−10455.
(17) Hsu, C.-C.; White, N. M.; Hayashi, M.; Lin, E. C.; Poon, T.; Banerjee, I.; Chen, J.; Pfaff, S. L.; Macagno, E. R.; Dorrestein, P. C. *Proc. Natl. Acad. Sci. U. S. A.* **2013**, *110*, 14855−14860.

DOI: 10.1021/acs.analchem.5b03389
Anal. Chem. 2015, 87, 11171−11175

(18) Sarsby, J.; Martin, N. J.; Lalor, P. F.; Bunch, J.; Cooper, H. J. *J. Am. Soc. Mass Spectrom.* **2014**, *25*, 1953−1961.
(19) Randall, E. C.; Bunch, J.; Cooper, H. *Anal. Chem.* **2014**, *86*, 10504−10510.
(20) Kiss, A.; Smith, D. F.; Reschke, B. R.; Powell, M. J.; Heeren, R. M. A. *Proteomics* **2014**, *14*, 1283−1289.
(21) Laskin, J.; Heath, B. S.; Roach, P. J.; Cazares, L.; Semmes, O. J. *Anal. Chem.* **2012**, *84*, 141−148.
(22) Lanekoff, I.; Heath, B. S.; Liyu, A.; Thomas, M.; Carson, J. P.; Laskin, J. *Anal. Chem.* **2012**, *84*, 8351−8356.
(23) LeDuc, R. D.; Taylor, G. K.; Kim, Y. B.; Januszyk, T. E.; Bynum, L. H.; Sola, J. V.; Garavelli, J. S.; Kelleher, N. L. *Nucleic Acids Res.* **2004**, *32*, W340−W345.
(24) Kim, S.; Lim, I. K.; Park, G.-H.; Paik, W. K. *Int. J. Biochem. Cell Biol.* **1997**, *29*, 743−751.
(25) Carpintero, P.; Anadón, R.; Díaz-Regueira, S.; Gómez-Márquez, J. *Neuroscience* **1999**, *90*, 1433−1444.
(26) Seeley, E. H.; Wilson, K. J.; Yankeelov, T. E.; Johnson, R. W.; Gore, J. C.; Caprioli, R. M.; Matrisian, L. M.; Sterling, J. A. *Bone* **2014**, *61*, 208−216.
(27) Hardesty, W. M.; Kelley, M. C.; Mi, D.-M.; Low, R. L.; Caprioli, R. M. *J. Proteomics* **2011**, *74*, 1002−1014.

DOI: 10.1021/acs.analchem.5b03389
Anal. Chem. 2015, 87, 11171−11175